AERATION PATHWAYS IN SOYBEAN ROOT NODULES

By F. J. BERGERSEN* and D. J. GOODCHILD*

[Manuscript received 12 December 1972]

Abstract

Soybean root nodule tissues contain many interconnected gas-filled intercellular spaces. They have been studied, in fresh and embedded tissue during the development and functional life of the nodules, by light and electron microscopy. Four anatomically different types of intercellular space were recognized in the bacteroid zone. These differed in distribution from the outside of the zone to the centre of the zone. There were fewer intercellular spaces in the outer cortex than in the bacteroid zone, but they were continuous and appeared to be adequate to conduct the observed fluxes of oxygen with only moderate differences in concentration between the outside of the bacteroid zone and the atmosphere. The observations suggested that aeration of the nitrogen-fixing tissue of mature nodules is accomplished primarily by radial gaseous diffusion from the external atmosphere through a network of 3,000–30,000 air-filled intercellular spaces per nodule in the cortex and up to 100,000 air spaces per nodule in the bacteroid zone, where each space has an average cross-sectional area of 1–5 μm^2.

I. INTRODUCTION

Legume root nodules require oxygen for the fixation of nitrogen (e.g. Burris *et al.* 1955). At the same time, oxygen inactives bacteroid nitrogenase (Bergersen 1968) and is an inhibitor of this system (Bergersen 1962*a*, 1962*b*; Wong and Burris 1972). For many legumes, oxygen at air concentration is insufficient to support maximum nitrogen-fixation rates by the nodules. Recently, evidence has been presented that leghaemoglobin, the characteristic haemoprotein of nitrogen-fixing legume root nodules, is involved in a mechanism which provides oxygen with an adequate flux, but at low concentration near the bacteroid surface (Tjepkema and Yocum 1970; Tjepkema 1971; Bergersen and Goodchild 1973); oxyleghaemoglobin rather than free oxygen may even be the terminal electron acceptor (Bergersen *et al.* 1973). Such a mechanism would operate within the enlarged host parenchyma cells which contain the bacteroids and the leghaemoglobin. These cells, together with a similar number of much smaller, uninfected, cells (interstitial cells), make up the cell matrix of the central "bacteroid zone" of the nodules. This zone is surrounded by cortical tissue which is supplied with vascular strands. It is necessary that oxygen should penetrate the cortical tissue and bacterial zone, but the pathways of penetration have been little studied. Tjepkema (1971) considered that there were insufficient intercellular spaces in the cortex where the resistance to diffusion was considered to be sufficient to cause the respiration of the central tissue of soybean nodules to be diffusion-limited.

* Division of Plant Industry, CSIRO, P.O. Box 1600, Canberra City, A.C.T. 2601.

In the present paper we present the results of a study of the nature, distribution, and dimensions of intercellular spaces in soybean nodules.

II. Materials and Methods

The nodule material examined was that which was produced in the main experiment of a companion paper (Bergersen and Goodchild 1973) and all of the results should be referred to the description of plant growth, nodule development, and activity described therein. For light microscopy, the same serial microtome sections stained by Heidenhain's haematoxylin–safranin were used for the quantitative studies of intercellular space distribution in nodule tissues, and the same electron micrographs were used for measurement of the space dimensions.

(*a*) *Microscopy*

Preliminary examination of the sections indicated that the intercellular spaces were oriented in predominantly radial directions through the nodule tissue, whose shape was approximately spherical. The orientation of the tissues used for the quantitative studies is described in Figure 1

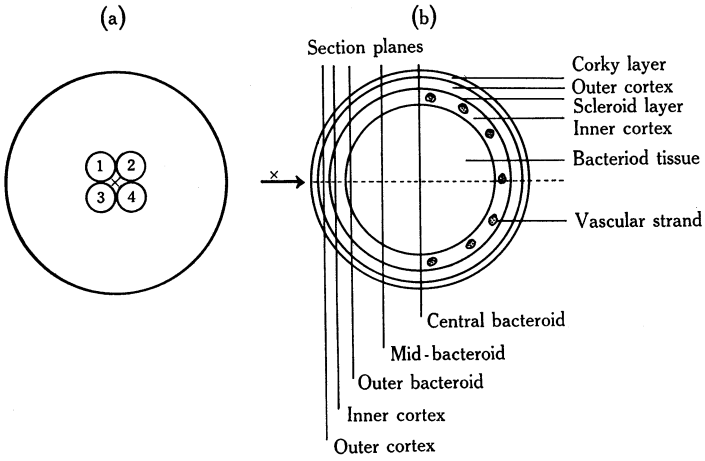

Fig. 1.—Diagrams of nodule tissue. (*a*) Showing the four microscope fields (0·023 mm²) clustered about the radial viewing axis X, which represents the centre of tangential sections. The frequencies of intercellular spaces were obtained from counts made in these four fields. (*b*) Identification of the nodule tissue zones and the positions of the planes of sections which were examined in the study of intercellular space distribution. The viewing axis, X, and the direction of observation are indicated by the arrow.

which also identifies the location of the various tissues and the terminology used to describe them. The direction of observation was approximately radial, using sections cut in planes parallel to an equatorial plane (tangential). Four microscope fields which were immediately adjacent to the centres of these sections were used for counting intercellular spaces [Fig. 1(*a*)]. In each of these fields, the viewing axis was approximately radial and parallel to the general viewing axis (X in Fig. 1).

For examination of air-filled spaces, fresh sections (100 μm thick) were cut from nodules and placed without added liquid on clean microscope slides. Moist chambers were formed around them by pieces of moistened filter paper each with a hole punched centrally. A cover slip, whose under surface was treated with an anti-fog preparation (Alston Safety Products, Melbourne), was rested on the paper, leaving a narrow air-gap above the nodule tissue. These preparations were examined by bright field illumination using $\times 20$ and $\times 40$ objectives.

Methods used in electron microscopy were those described elsewhere (Goodchild and Bergersen 1966; Bergersen and Goodchild 1973). Areas of intercellular space cross-sections were measured by cutting out and weighing photographic profiles of accurately known magnification. Shrinkage was estimated from measurement of sides of tissue cubes before and after dehydration and embedding and by comparison of fresh tissue cell dimensions with those in sections. Wax-embedded tissue shrank by 20–30% according to nodule age, but tissue cut into 1-mm cubes and embedded for electron microscopy shrank less (10–15%). Estimates of intercellular space cross-sections in electron micrographs therefore underestimated the areas by 20–30%. Because these factors are not accurately known for the actual sections examined, areas have not been adjusted for shrinkage.

III. Results

Soybean nodules are spheroidal bodies (Figs. 2*A*, 2*B*) which are connected to the root at slightly flattened bases where the vascular traces fuse and pass into the root to connect with the stele. The main tissues are illustrated by the micrograph of a wax-embedded section in Figure 2*B*.

(*a*) *Presence of Gas in the Intercellular Spaces*

Examination of fresh sections in air at low magnification showed that all tissues were traversed by a network of dark lines (Figs. 3*A*, 3*B*). At higher magnifications (Figs. 3*C*, 3*D*), these lines were revealed as spaces whose edges were darker than the middle (a bubble of air trapped in water between coverslip and slide is dark at the edges and lighter in the centre when viewed with similar illumination). The dark spaces disappeared from the surfaces of sections, and became discontinuous within them, when they were infiltrated with water. It was concluded that these were gas-filled intercellular spaces. They were predominantly radial in direction, but cross-connections were frequent. By careful focusing, it could be seen that the spaces ran between the cells and frequently between elongated bacteroid-filled cells and adjacent lines of interstitial cells. In the inner cortex, the spaces connected with one another and in the outer cortex they connected with large gaps between stacks of corky outer tissue. The only tissue where interconnecting spaces were difficult to see was in parts of the discontinuous, single-cell-deep, scleroid cell layer which divided the inner and outer cortex (Fig. 2*B*). Air spaces could be seen but tracing their continuity between the spaces of the inner and outer cortex was difficult because of the large irregular scleroid cells. In spite of this difficulty, connections were observed and we concluded that there were continuous interconnected gas-filled spaces from the outside to the centre of the nodules at all ages. Intercellular spaces were less frequent close to vascular traces. We also observed that very few, if any, intercellular spaces were not gas-filled.

(*b*) *Numbers and Distribution of Intercellular Spaces*

Microtome sections of wax-embedded nodules were examined according to the orientation shown in Figure 1. The micrographs of wax-embedded sections shown in Figures 4*A*–4*C* illustrate intercellular spaces in the cortex. Figures 4*D*–4*G* show the types of intercellular space which could be recognized in the bacteroid zone. Type *a* was bounded by the walls of adjacent bacteroid-containing cells; type *b* by the walls of two bacteroid-containing cells and one interstitial cell; type *c* by the

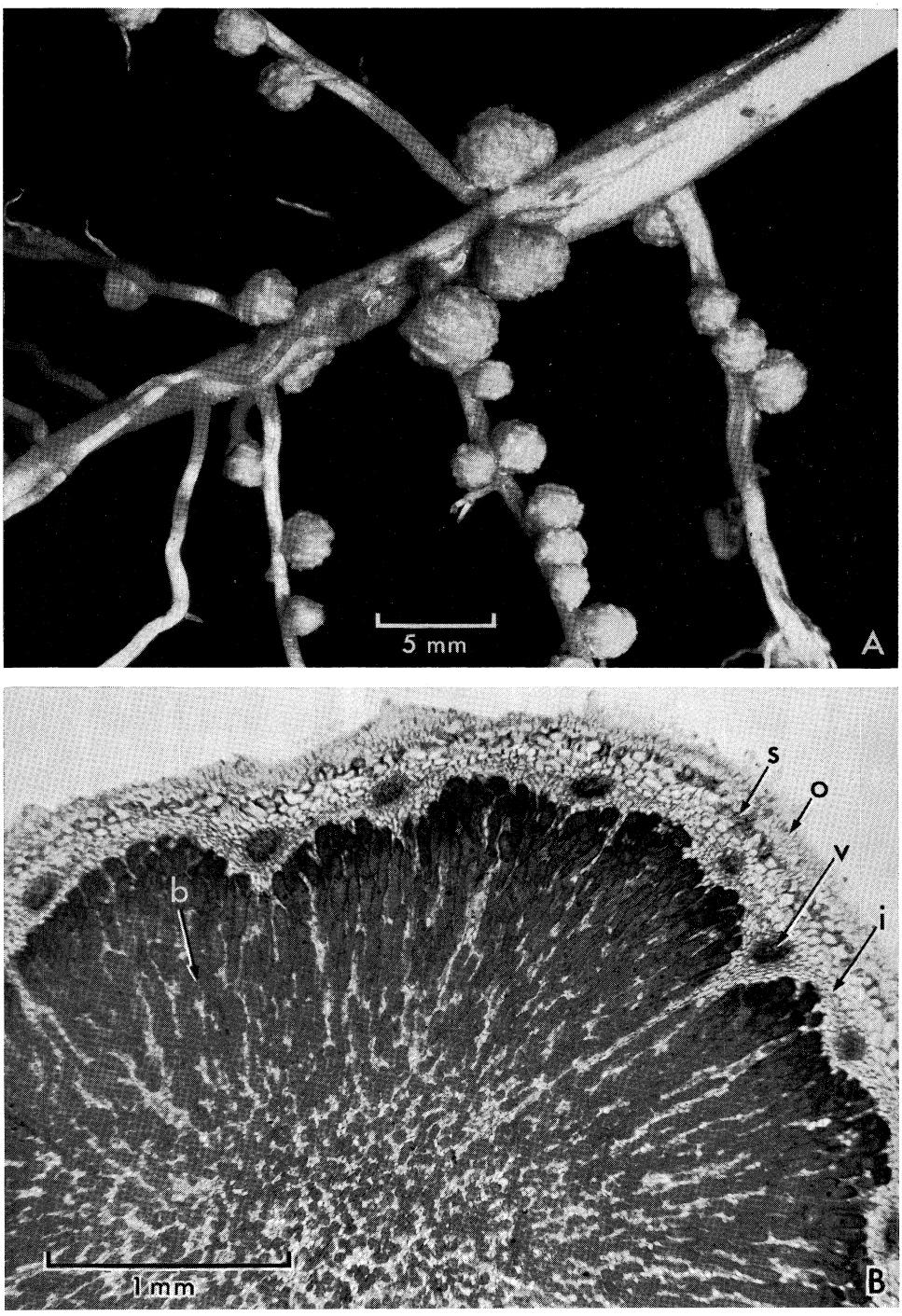

Fig. 2.—*A*, external appearance of soybean root nodules. Note the approximately spherical shape. *B*, part of a median section of a nodule aged 43 days. The complete section is approximately circular. The main tissues are shown: *o*, outer cortex; *i*, inner cortex; *s*, layer of scleroid cells; *v*, vascular trace; *b*, bacteroid zone showing increased frequency of interstitial cells near the centre of the zone (the darkly stained, large cells contain bacteroids).

walls of two interstitial cells and one bacteroid-containing cell, and type *d* was found between the walls of adjacent interstitial cells only. Figure 4*H* shows the arrangement of these intercellular spaces in a phase-contrast light micrograph of a 0·15 μm-thick section of plastic-embedded nodule tissue prepared for electron microscopy.

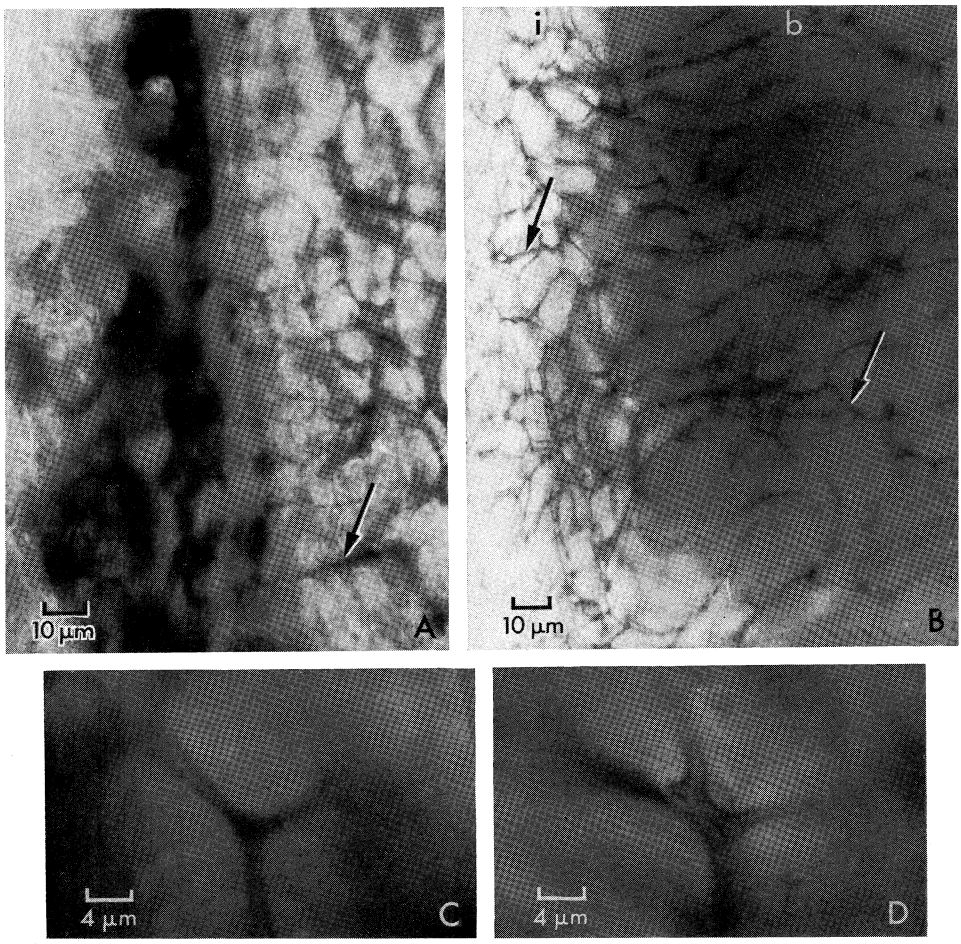

Fig. 3.—Air-filled intercellular spaces in unstained, fresh nodule sections. The spaces show as dark lines or areas. Arrows indicate spaces which are continuous across the entire tissue zone. *A*, air-filled spaces in the corky outer cortex. The nodule exterior is on the left and the scleroid layer is to the right. *B*, air-filled spaces in the inner cortex (*i*) communicating with spaces in the bacteroid zone (*b*). The leghaemoglobin in the bacteroid zone shows as a dark overall shading. *C* and *D*, higher magnifications of air-filled spaces in the bacteroid zone.

The numbers of intercellular spaces per microscope field remained approximately constant in each tissue zone, as the nodules increased in age and size. They were more frequent, by a factor of about 4, in the bacteroid zone than in the cortical tissues (Table 1). Table 2 gives the absolute numbers of spaces presented to the outer surfaces of each tissue zone. The bacteroid zone was regarded as a sphere with the

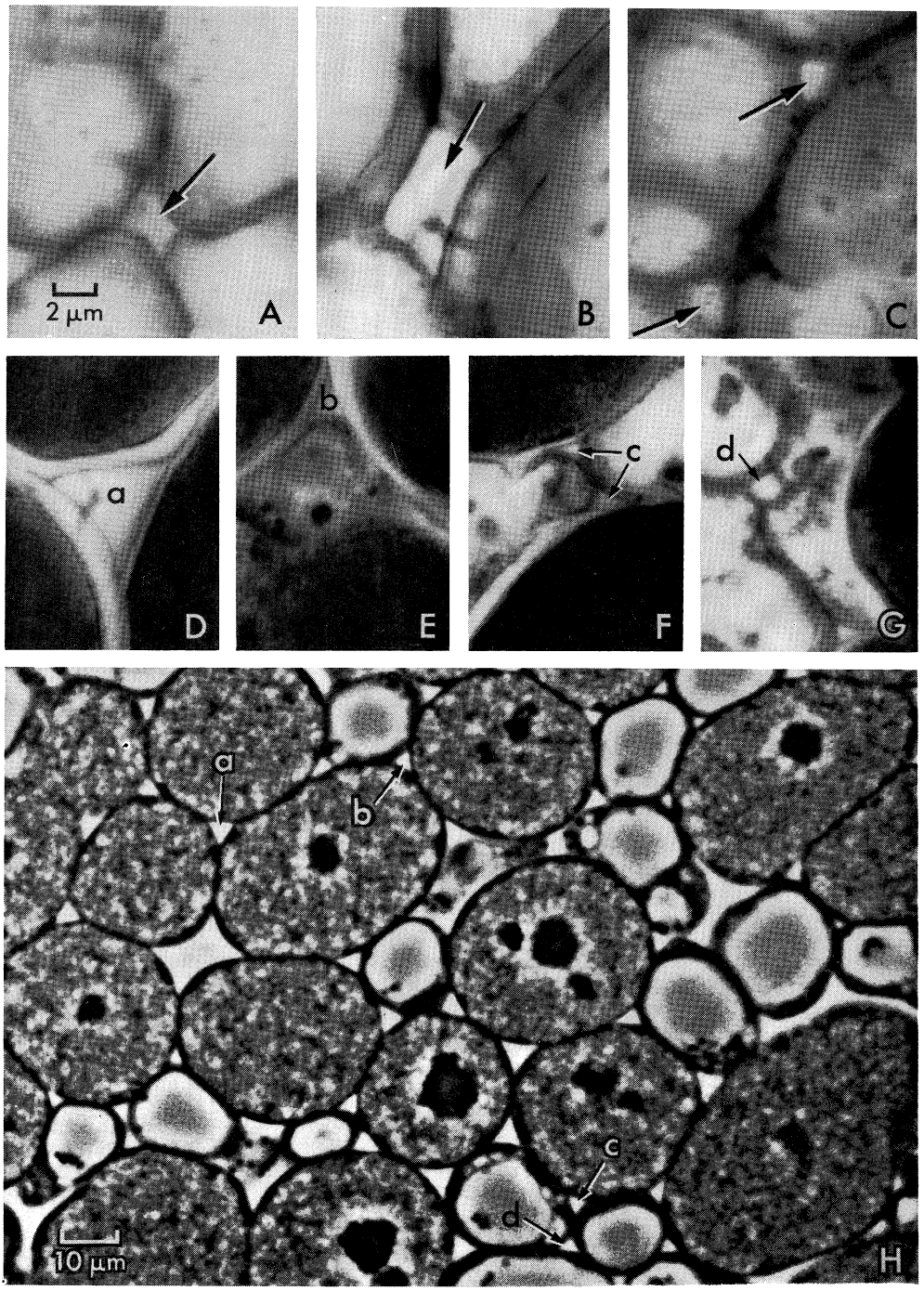

Fig. 4.—Types of intercellular spaces (arrowed) observed in radial directions in sections of various nodule tissues. Micrographs *A–G* all have the magnification indicated on *A*, and are wax-embedded sections stained by Heidenhain's haematoxylin: *A*, outer cortex; *B*, between scleroid cells; *C*, inner cortex; *D–G*, bacteroid zone. Space types *a*, between three bacteroid cells, *b*, between

two cortical zones as shells around it, for the purposes of these calculations. In the cortical zones the numbers of spaces increased approximately 10-fold during growth

TABLE 1

NUMBERS OF INTERCELLULAR SPACES IN MICROSCOPE FIELDS (0·023 mm²) OF TANGENTIAL SECTIONS THROUGH VARIOUS TISSUE ZONES OF NODULES OF VARIOUS AGES

Nodule age (days)	Mean number of intercellular spaces per microscope field*				
	Outer cortex	Inner cortex	Outer bacteroid zone	Mid-bacteroid zone	Centre bacteroid zone
8	10·6	8·3	37·5	50·6	50·4
15	10·1	10·8	33·8	44·2	46·8
22	9·8	11·9	43·3	42·9	46·8
30	9·6	11·3	41·2	45·6	48·6
43	11·0	10·3	38·6	40·6	38·6
Mean±S.E.†	10·0±2·2	10·7±3·1	39·1±11·6	44·8±8·1	46·5±10·1

* From 8 to 12 fields counted from each zone at each age.
† All fields, all ages.

TABLE 2

NUMBERS OF INTERCELLULAR SPACES (IN THOUSANDS) IN OUTER SURFACES OF VARIOUS TISSUE ZONES OF SOYBEAN NODULES WITH INCREASING AGE

D, average median section diameter; *R*, radius

Nodule age (days)	*D* (mm)	Outer cortex		Inner cortex		Bacteroid zone	
		R (mm)	Spaces/ nodule*	*R* (mm)	Spaces/ nodule*	*R* (mm)	Spaces in outer* zone surface
5	1·35	0·67	3·2	0·58	2·1	0·52	5·2
8	2·30	1·15	7·8	1·00	5·5	0·87	15·1
15	3·19	1·59	14·4	1·42	11·8	1·30	28·4
22	3·56	1·78	16·2	1·66	17·9	1·52	53·9
30	4·02	2·01	25·2	1·98	25·5	1·86	79·7
43	4·87	2·44	30·4	2·26	25·4	2·12	98·7

* The intercellular spaces counted per microscope field in the outer bacteroid-containing zone have been used to calculate the numbers of intercellular spaces presented to the outside surface of this zone. The other zones are in fact shells and the numbers of spaces also here relate to the outer surface of the zones.

in nodule diameter from 1·35 mm to 4·87 mm. In the bacteroid zone the increase was about 20-fold.

two bacteroid cells and an interstitial cell; *c* between two interstitial cells and a bacteroid cell; *d*, bounded on all sides by interstitial cells. *H*, plastic-embedded section from a block prepared for electron microscopy. *a*, *b*, *c*, *d*, indicate the four types of intercellular space in the bacteroid zone. Phase-contrast illumination.

In the bacteroid zone, type *a* intercellular spaces decreased in frequency from the outside of the zone to the centre, while types *c* and *d* increased (Fig. 5). This was due to the increased proportion of interstitial cells towards the centre of the bacteroid zone (Table 3).

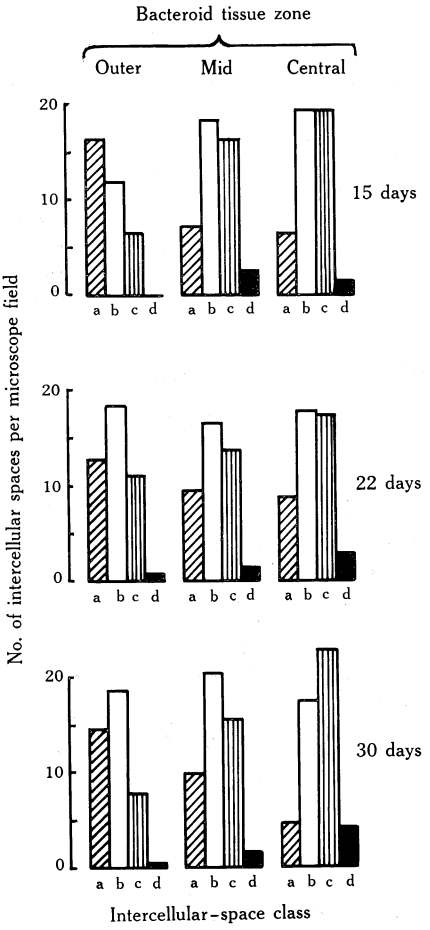

Fig. 5.—Distributions of types of intercellular spaces in three parts of the central tissue zone of nodules aged 15, 22, and 30 days. For identification of the four types of space, see the text and Figures 4*D*–4*G*.

(*c*) *Dimensions of the Intercellular Spaces*

Cross-sectional areas of the intercellular spaces in the bacteroid zone were measured from selected electron micrographs in which the planes of the sections appeared to be transverse to the longitudinal axis of the space (Fig. 6). The measurements were very variable, and with one exception, the areas increased with age. The mean values were in the range 1–5 μm^2 (Table 4). In wax sections of cortical tissues the ranges of sizes were greater (0·2–9 μm^2) but the averaged values were similar. The variability and unknown shrinkage compared with the electron micrographs prevented more accurate estimation of the cross-sectional areas of spaces in the cortex. Dissection of micrographs of the bacteroid zone showed that intercellular spaces accounted for 2·4, 2·9, 2·4, 3·6, 4·0, 5·0, and 5·1% of the nodule bacteroid zone space at 5, 10, 15, 22, 30, 36, and 43 days of nodule age respectively.

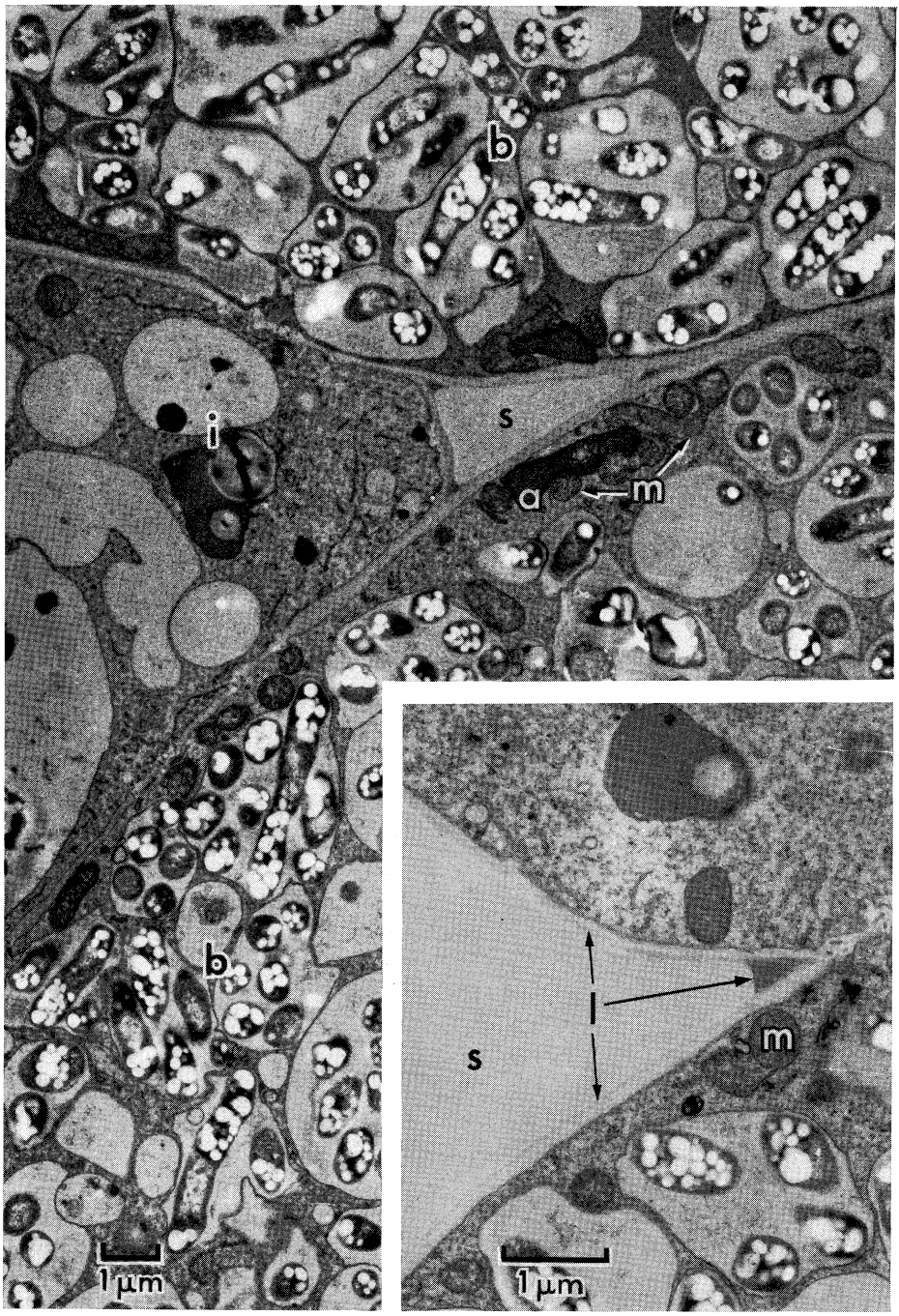

Fig. 6.—An electron micrograph showing bacteroid-containing cells (*b*) with mitochondria (*m*) and amyloplasts (*a*) concentrated in the periphery of the cell adjacent to an intercellular space (*s*), which is bounded on one side by an interstitial cell (*i*). *Inset:* An electron-dense layer (*l*) can be seen extending from the corners to line the inner surface of the cell walls around the space.

(*d*) *Electron Microscopy of Intercellular Spaces in the Bacteroid Zone*

Examination of electron micrographs of sections of the bacteroid zone showed that the peripheries of bacteroid-containing cells adjoining intercellular spaces were

TABLE 3

INCREASED FREQUENCY OF INTERSTITIAL CELLS TOWARDS THE NODULE CENTRE

Ratio of the number of interstitial cells per field to number of bacteroid cells per field estimated and mean values given for *n* determinations. As there were no significant differences among the values for various ages in any zone, ratios for all ages were pooled and the differences analysed

Nodule age (days)	Ratio		
	Outer central zone	Mid-central zone	Centre of central zone
5	0·56	0·56	1·24
8	0·60	0·94	1·98
15	0·36	1·23	1·33
22	0·62	0·72	1·70
30	0·51	0·93	1·82
43	0·99	1·09	1·60
Mean ± S.E. (all ages)	0·62 ± 03·8	0·99 ± 0·38	1·61 ± 0·62
n	43	52	51
P	<0·001	<0·001	

TABLE 4

CROSS-SECTIONAL AREAS OF INTERCELLULAR SPACES OF THE BACTEROID ZONE OF SOYBEAN ROOT NODULES

Areas were obtained from electron micrographs, selected for orientation, and with known final magnification. Intercellular space profiles were cut out, weighed, and the print areas calculated from a weight–area calibration. Print areas were then reduced to actual area by dividing by the square of the magnification. The values given are not corrected for shrinkage during embedding

Nodule age (days)	Space class *a* area (μm^2)			Space class *b* area (μm^2)			Space class *c* area (μm^2)		
	Mean	S.D.	Range	Mean	S.D.	Range	Mean	S.D.	Range
8	1·3	0·6	0·6–2·1	1·5	0·7	0·3–2·0	0·9	0·4	0·5–1·4
15	2·6	1·5	1·2–4·6	2·2	1·2	0·6–3·6	1·8	1·7	0·6–3·1
22	4·3	0·5	3·9–4·6	5·0	3·0	0·5–8·2	2·3	0·9	1·2–3·8
30	4·5	2·8	1·3–8·6	1·5	1·3	0·6–3·3	3·1	2·0	0·8–6·2

invariably enriched in mitochondria and amyloplasts (Fig. 6). All traces of starch had disappeared from these amyloplasts when the nodules were older than 5 days. In contrast, mitochondria and amyloplasts seemed to be randomly distributed in the

interstitial cells, and starch was observed within amyloplasts in these cells at all nodule ages. In young nodules (5–15 days) the lumen of intercellular spaces appeared to be lined with a membrane-like layer, which was detached from the cell wall surface in some sections. In older nodules (Fig. 6) this layer appeared as electron-dense material in the corners of the space profiles, extending to a thin layer lining the lumen of the space.

IV. Discussion

The data presented in this paper allow the following generalizations about the diffusion of oxygen into nodule tissues. Firstly, the diffusion of oxygen is probably gaseous, via intercellular spaces from the external atmosphere to the surfaces of all respiring plant cells, as indicated from light microscope observations of fresh sections. Higher rates of diffusion are thus possible than would be the case if substantial aqueous phase diffusion was involved. These results are in agreement with Sprent (1972), who considered that the spaces were air-filled, but the gas-filled space (2·4–5% of the bacteroid zone space) is not as large as estimated by this author (25%), who measured the volume of gas produced by decompression of nodules.

Secondly, it is unlikely that restricted air passages through the cortex are the main source of diffusion resistance, as suggested by Tjepkema (1971), who assumed that there were no continuous gas passageways between the soil atmosphere and the central tissue. Our microscopic observations of sections of fresh nodule tissue showed the presence of continuous gas passageways of this type. This is confirmed by the observation that slight decompression (about 0·5 atm, which promotes only slow release of gas from solution) of intact nodules immersed in water, allows minute bubbles of gas to escape from many points on the surface (cf. Sprent 1972). We also calculated that the size and number of intercellular spaces seen in the cortex were adequate to allow the passage, by gaseous diffusion, of the amounts of oxygen reported to be respired by nodules of these ages (Bergersen 1962*a*, 1962*b*; Tjepkema 1971), with the development of only minor differences in concentration between the outer atmosphere and the inner surface of the cortex.

Thirdly, the gradients of p_{O_2} within the intercellular air spaces of the bacteroid zone may not be extreme in the innermost tissue because the frequency of the spaces (number per microscope field, Table 1) is fairly constant from the outer surface to the centre of the zone, while the frequency of the bacteroid-containing cells (which must represent major sinks for oxygen-uptake) falls in absolute terms and in relation to numbers of interstitial cells (Table 3). The increases in intercellular space cross section area (Table 4) which occur with increasing age, tend to compensate for the increased length of the diffusion path as the nodule radius increases.

Fourthly, the presence of large numbers of plant cell mitochondria adjacent to the intercellular spaces (e.g. Fig. 6) would compete effectively with leghaemoglobin and bacteroids for oxygen penetrating from the intercellular spaces into the bacteroid-filled cytoplasm of the central tissue cells, if the oxidases of these mitochondria are much less than saturated with respect to oxygen.

It is therefore proposed that the host cells in the cortex, the central tissue interstitial cells, and the mitochondria at the periphery of the bacteroid-containing

cells represent a continuum of oxygen sinks which may be the equivalent of the "cortex" in the considerations of Tjepkema (1971). The progressive saturation of these sinks with increasing p_{O_2} may account for the inflection which is sometimes observed in nodule respiration/p_{O_2} curves (Bergersen 1962*a*; Tjepkema 1971). Increases in p_{O_2} beyond this inflection [above about 0·4–0·5 atm, in Bergersen (1962*a*) and above about 0·3 atm in Tjepkema (1971)], may represent more sharply increasing saturation of the bacteroid–leghaemoglobin system. This was demonstrated in the sharply increased oxygenation of the leghaemoglobin above p_{O_2} of 0·5 atm which was observed in earlier work (Bergersen 1962*b*).

We have not attempted a mathematical evaluation of these proposals because of the unknown relationship between oxygen and oxyleghaemoglobin concentrations and rates of bacteroid oxygen consumption. An understanding of this relationship would be essential before an analysis of oxygen flux within the gas spaces of this tissue could be realistically attempted.

The maintenance of the gas-filled spaces in nodules when the tissue is fully turgid and the nodules are in contact with free water in the soil suggests that the intercellular spaces may be lined with water-repellent material. The electron-dense material observed in corners of intercellular space profiles in electron micrographs and extending to a very thin layer lining the lumen of the space (Fig. 6) may represent a water-repellant layer.

VI. Acknowledgments

The authors acknowledge the skilled assistance of Mrs. M. A. Jeppersen in this work.

VI. References

Bergersen, F. J. (1962*a*).—The effects of partial pressure of oxygen upon respiration and nitrogen fixation by soybean root nodules. *J. gen. Microbiol.* **29**, 113–25.

Bergersen, F. J. (1962*b*).—Oxygenation of leghaemoglobin in soybean root nodules in relation to the external oxygen tension. *Nature, Lond.* **194**, 1059–61.

Bergersen, F. J. (1968).— The symbiotic state in legume root nodules; studies with the soybean system. Trans. IXth Int. Congr. Soil Sci. Vol. 2. pp. 49–63.

Bergersen, F. J., and Goodchild, D. J. (1973).—The cellular location and concentration of leghaemoglobin in soybean root nodules. *Aust. J. biol. Sci.* **26**, 741–56.

Bergersen, F. J., Turner, G. L., and Appleby, C. A. (1973).—Studies on the physiological role of leghaemoglobin in soybean root nodules. *Biochim. biophys. Acta* **292**, 271–82.

Burris, R. H., Magee, W. E., and Bach, M. K. (1955).—The pN_2 and the pO_2 function for nitrogen fixation by excised soybean nodules. *Ann. Acad. Sci. Fenn.* **60**, 190–9.

Goodchild, D. J., and Bergersen, F. J. (1966).—Electron microscopy of the infection and subsequent development of soybean nodule cells. *J. Bact.* **92**, 204–13.

Sprent, J. I. (1972).—The effects of water stress on nitrogen fixing root nodules. II. Effects on the fine structure of detached soybeans. *New Phytol.* **71**, 443–50.

Tjepkema, J. D. (1971).—Oxygen transport in the soybean nodule and the function of leghaemoglobin. Ph.D. Thesis, University of Michigan, U.S.A.

Tjepkema, J. D., and Yocum, C. S. (1970).—Leghaemoglobin facilitated oxygen diffusion in soybean nodule slices. *Pl. Physiol., Lancaster* **46** (Suppl.), 44.

Wong, L. X., and Burris, R. H. (1972).—Nature of oxygen inhibition of nitrogenase from *Azotobacter vinelandii*. *Proc natn. Acad. Sci. U.S.A.* **69**, 672–5.